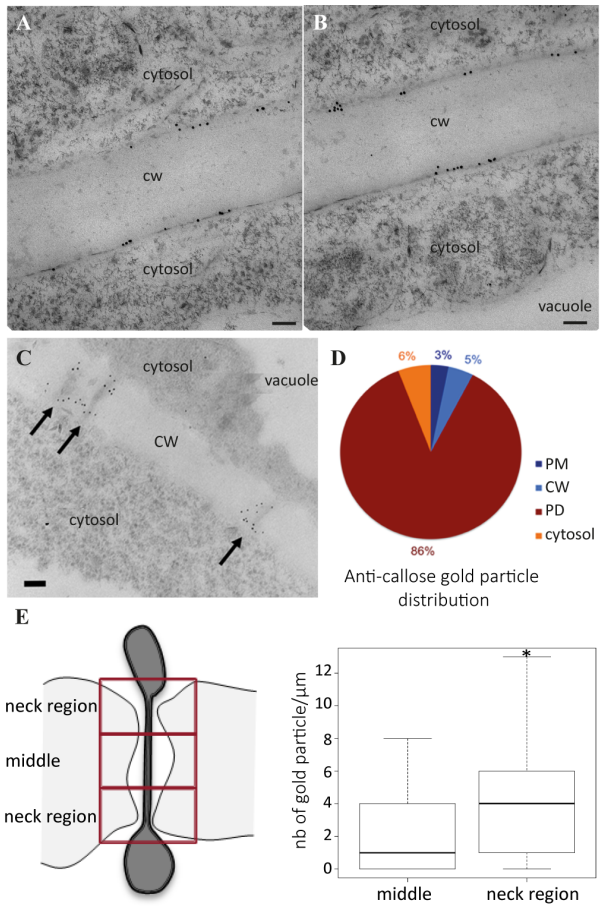

Supplemental Figure 1.

Immunogold labelling of PMA2 and callose in cryo-substituted Arabidopsis suspension cells.

(A, B) PMA2 immunogold labelling (10 nm gold particles) showing that the proton pump ATPase is tightly associated with the PM. Scale Bars= 100 nm

(C) Callose immunogold labelling (5 nm gold particles) showing that callose is mainly associated with PD (arrows). Scale Bar= 100 nm

(D) Quantification of callose gold particle distribution at the PM, cell wall (CW), PD and cytosol (n=222 gold particles from 32 micrographs).

(E) Quantification of callose gold particle distribution along the PD channels. Micrographs with PD channels visible from neck to neck were selected and gold particle association with either the PD orifice or PD central region estimated (channels were divided into three identical regions of interest). The number of gold particles associated with the neck region was slightly higher than for the central region (n= 210 and 71 gold particles for neck and central region respectively; from 31 micrographs). Asterisks indicate a significant difference ($p < 0.05$ for one asterisk) by Wilcoxon test.

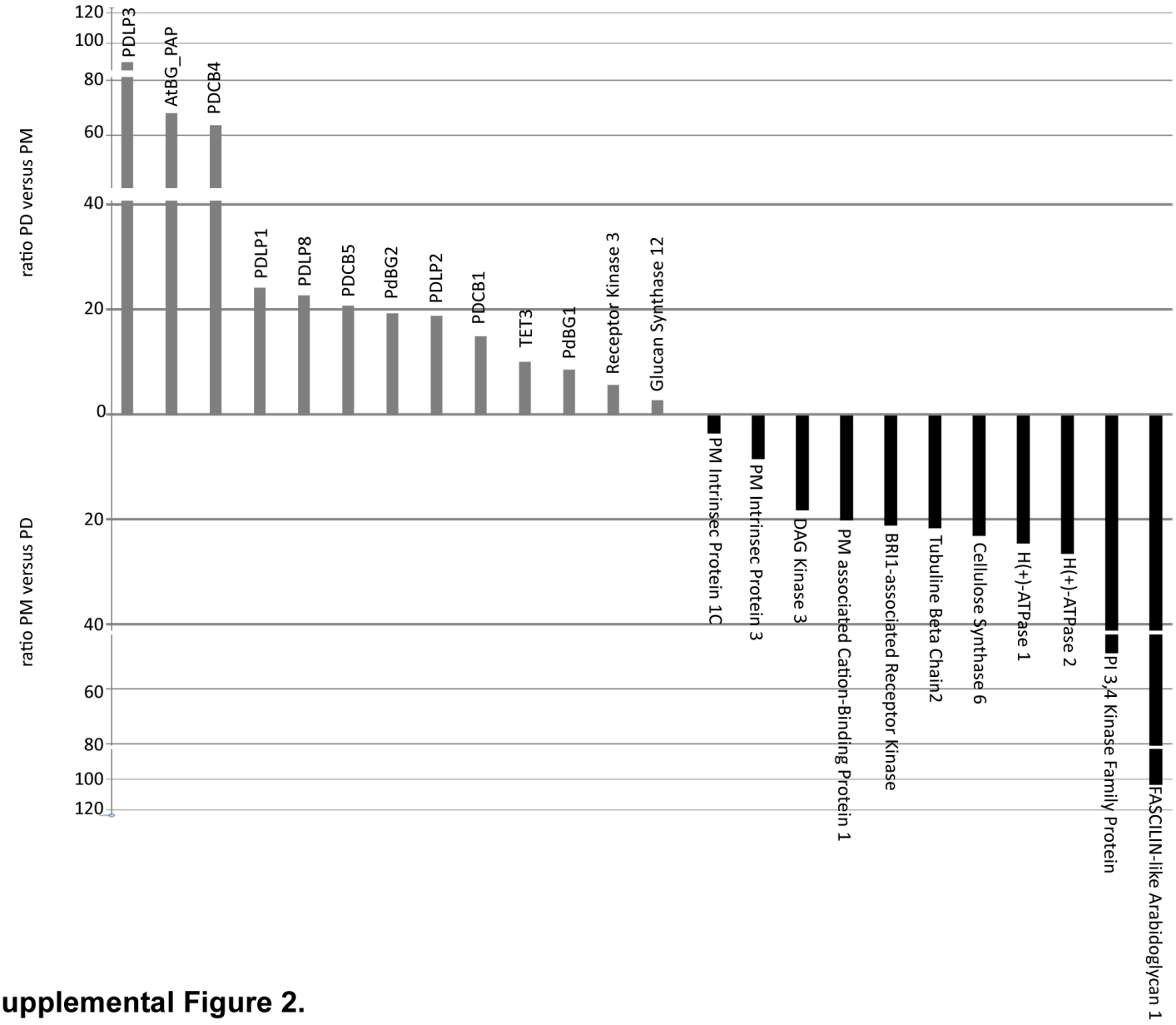

Supplemental Figure 2.

Quantitative proteomic analysis reveals that PD-associated proteins are highly enriched in the PD fraction compared to the bulk PM.

Ten micrograms of PD and PM fractions were subjected to proteomic analysis after trypsin digestion by LC/MS/MS (n=3). The relative abundance of specific proteins was compared between the two samples after summing the signal intensity of their individual peptides. Known PD-associated proteins are greatly enriched in the PD fraction when compared to the PM (gray). By contrast classical PM proteins show consequential depletion (black).

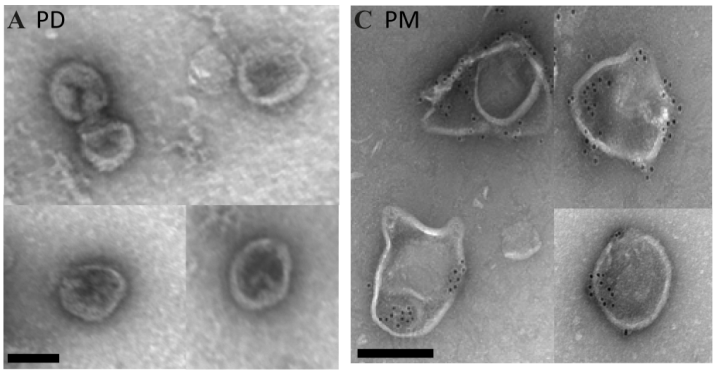

Supplemental Figure 3.

Immunogold labelling of PMA2 on purified PD and PM fractions.

Electron micrograph of PMA2 immunogold labelling of the PD **(A)** and PM **(C)** fractions showing that PMA2 heavily labels PM but not PD-enriched membrane vesicles. The density of gold particles per vesicle (**B** and **D**) was calculated for both negative control (n=82 vesicles for PD and n=93 for PM) and specific anti-serum (n=61 vesicles for PD and n=114 for PM). Scale Bar= 50 nm for A and 200 nm for B.

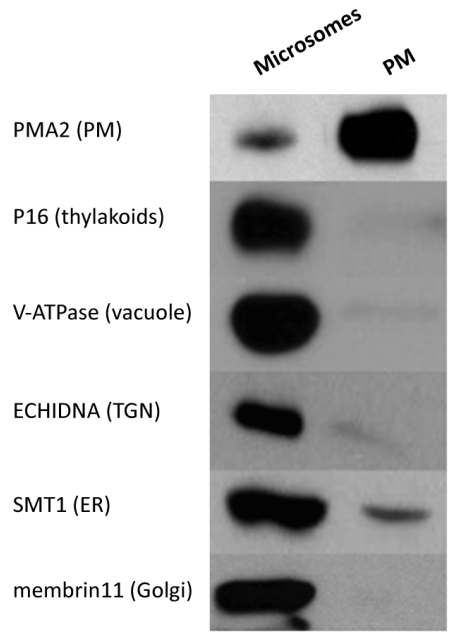

Supplemental Figure 4.

Purity assessment of the PM fraction by immunoblot analyses.

Compared to the microsomal fraction, the PM fraction is enriched for the PM marker PMA2 while strongly depleted in integral membrane proteins of the thylakoids (P16), vacuole (V-ATPase), trans-Golgi network (TGN) (ECHIDNA), endoplasmic reticulum (ER) (SMT1) and Golgi apparatus (Membrin11). The same amount of proteins (8 µg) was loaded in each lane.

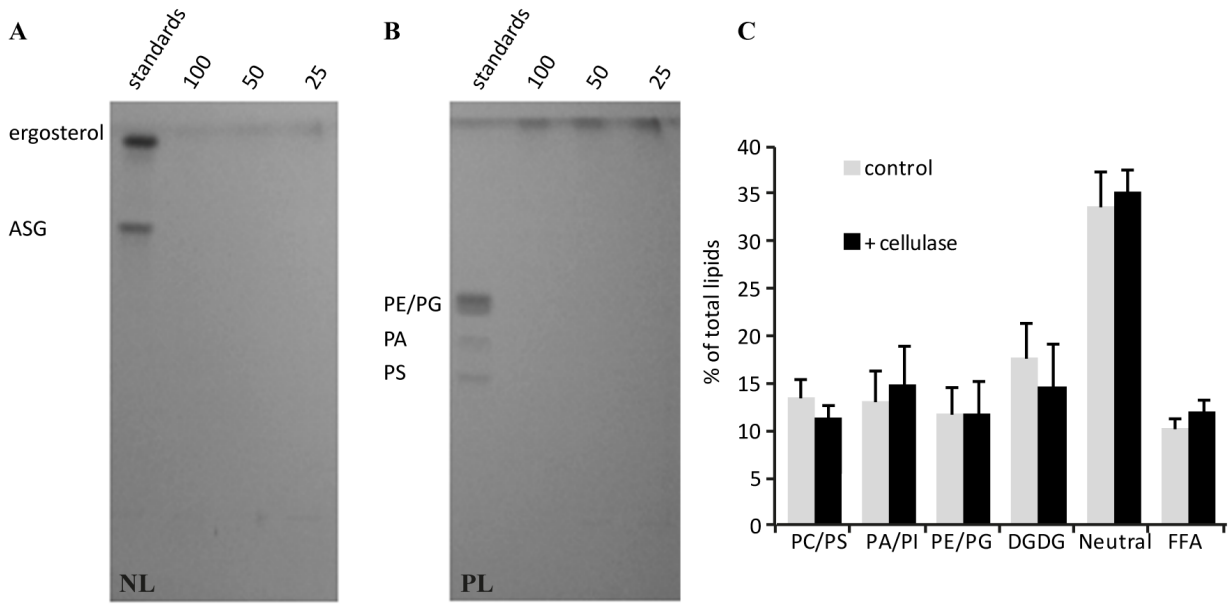

Supplemental Figure 5.

The cellulase solution used for PD isolation does not contain lipids or lipase activity.

(A, B) HP-TLC migration for neutral lipids (NL) (A) and polar lipids (PL) (B). The cellulase powder (100, 50 and 25 mg) used in the PD purification procedure was subjected to lipid extraction and loaded on HP-TLC plates. Note that no lipids were detected.

(C) Membrane fractions (n=4) obtained from Arabidopsis suspension cells were subjected to cellulase treatment using the same experimental procedure as for the purification of PD. Lipids extracted from control membranes and cellulase-treated membranes were separated by HP-TLC and lipids quantified by densitometric scanning. Note that no significant differences were observed between the two sets (Wilcoxon statistical test). DGDG: digalactosyldiacylglycerol, FFA: free fatty acids, PA: phosphatidic acid, PC: phosphatidylcholine, PE: phosphatidylethanolamine, PG: phosphatidylglycerol, PI: phosphatidylinositol, PS: phosphatidylserine. Bars indicate SD.

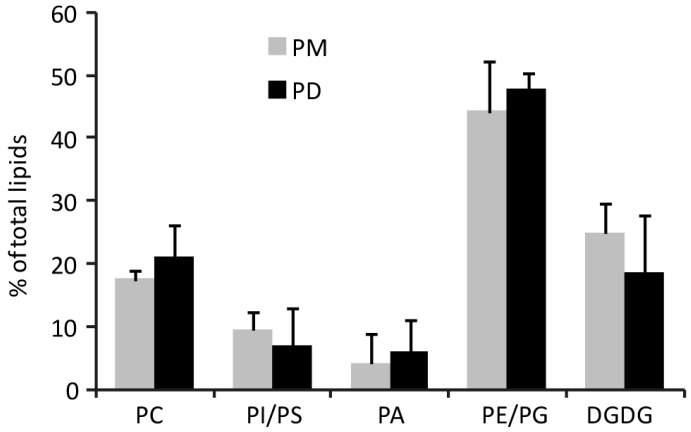

Supplemental Figure 6.

Quantification by HP-TLC of the different glycerolipid classes from isolated PD and PM fractions from Arabidopsis suspension cells.

Lipids were separated by HP-TLC and after staining, quantified by densitometry scanning. Note that the glycerolipid profile is not significantly different between PD and PM samples (Wilcoxon statistical test). DGDG: digalactosyldiacylglycerol, PA: phosphatidic acid, PC: phosphatidylcholine, PE: phosphatidylethanolamine, PG: phosphatidylglycerol, PI: phosphatidylinositol, PS: phosphatidylserine. n=5 for PM and PD. Bars indicate SD.

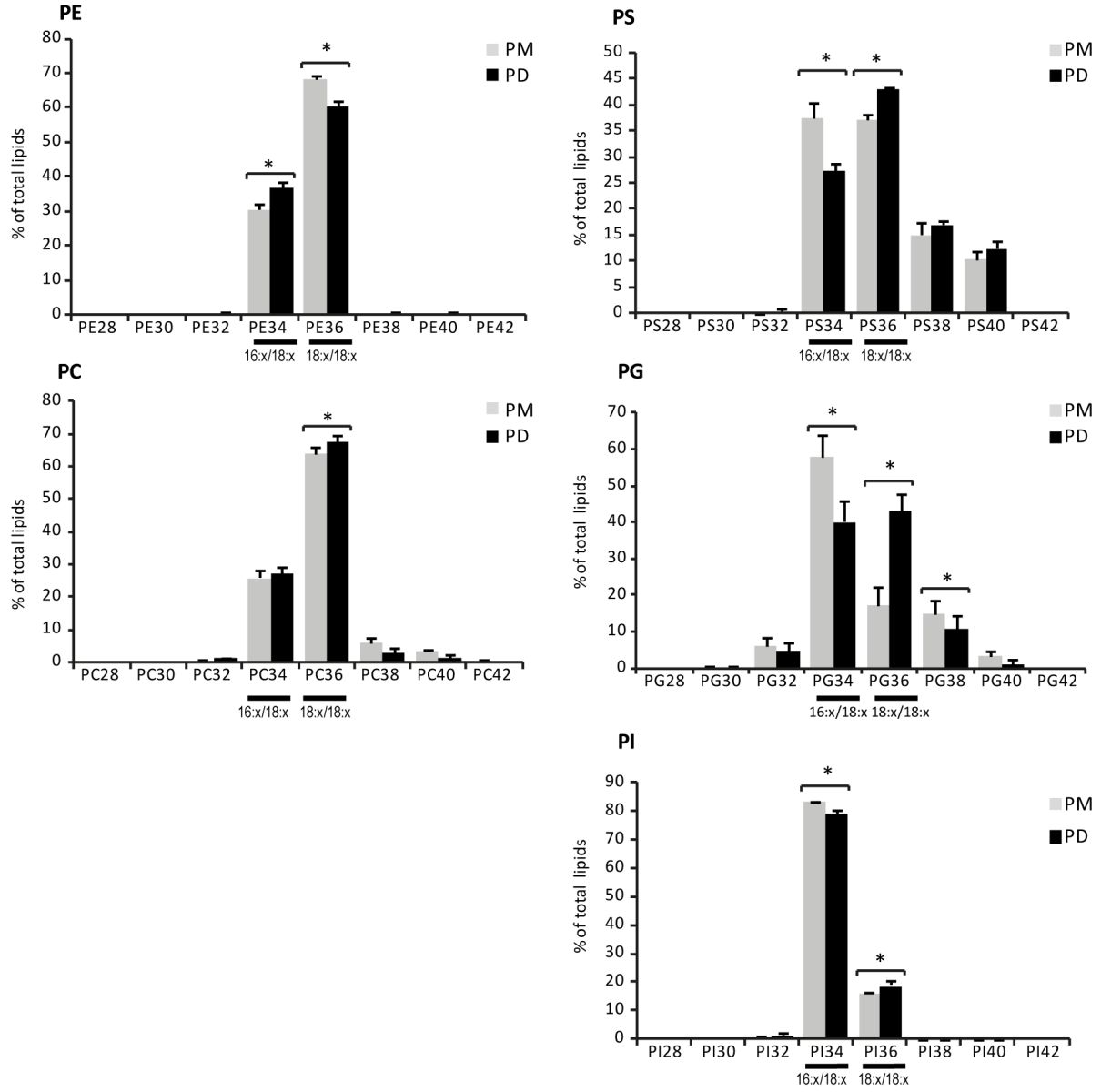

Supplemental Figure 7.

Quantification by LC-MS/MS of the phospholipid molecular species associated with the PD and PM fractions from Arabidopsis suspension cells.

All phospholipid classes analysed (PC: phosphatidylcholine, PE: phosphatidylethanolamine, PG: phosphatidylglycerol, PI: phosphatidylinositol, PS: phosphatidylserine), are primarily composed of the long chain molecular species C34 and C36. These molecular species contain fatty acids of 16 or 18 carbon atoms (saturated or unsaturated) depicted as 16:x or 18:x. n=3 for PD and n=4 for PM. Asterisks indicate a significant difference ($P < 0.05$) between two samples by Annova of Kruskal-Wallis test. n=3 for PD and n=4 for PM. Bars indicate SD.

For each phospholipid class, individual molecular species are expressed as a percentage of total phospholipid molecular species found in this class.

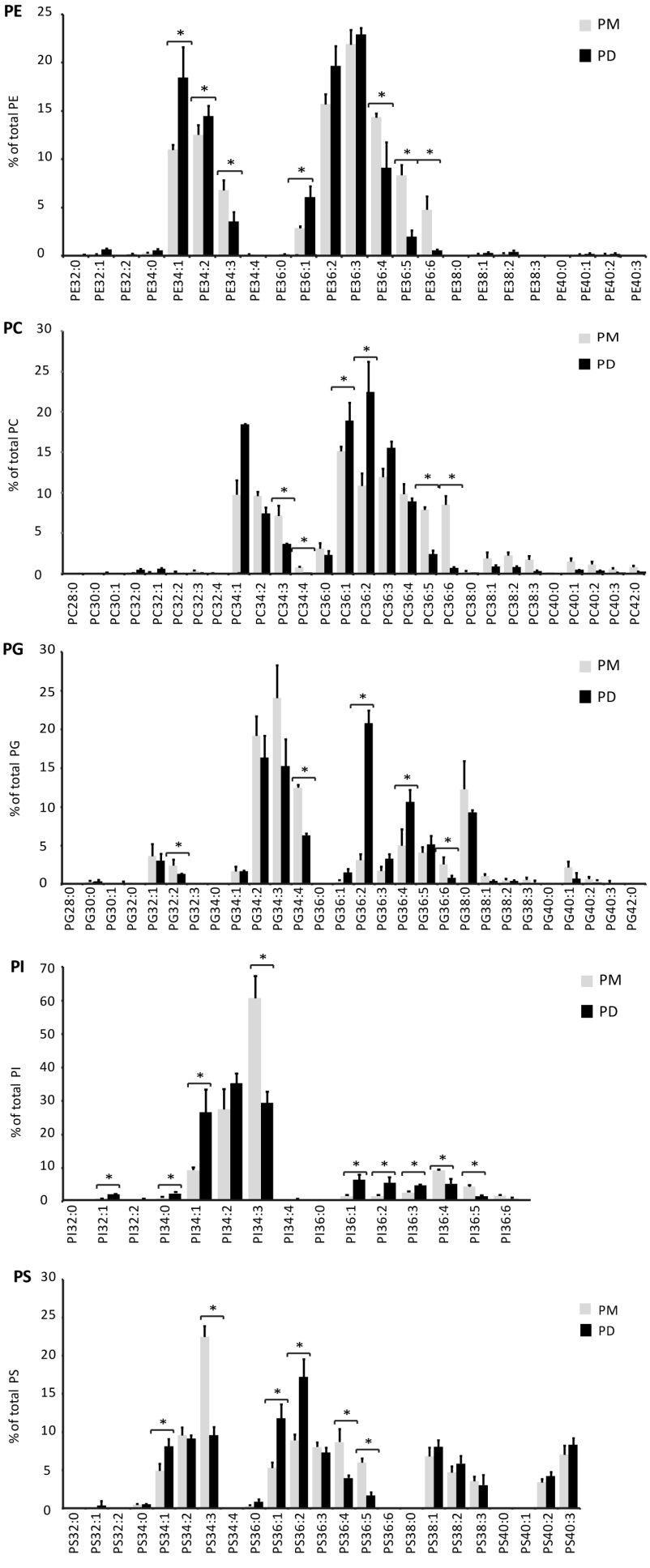

Supplemental Figure 8 online.

Molecular composition of phospholipid species identified by LC-MS/MS.

PC: phosphatidylcholine, PE: phosphatidylethanolamine, PG: phosphatidylglycerol, PI: phosphatidylinositol, PS: phosphatidylserine. Asterisks indicate a significant difference ($P < 0.05$) between two samples by Annova of Kruskal-Wallis test. n=3 for PD and n=4 for PM. Bars indicate SD.

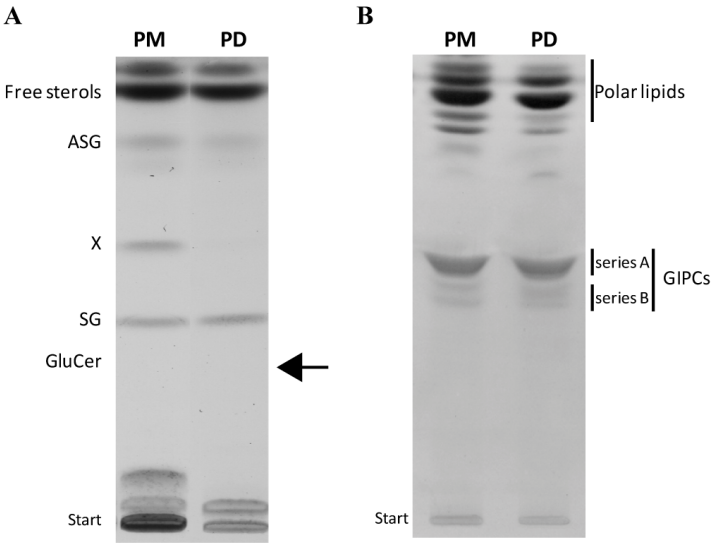

	GIPCs series A (total GIPCs %±sd)	GIPCs series A (total GIPCs %±sd)
PM	70±5	30±5
PD	69±12	31±12

Supplemental Figure 9.

The complex sphingolipids GIPCs constitute the major sphingolipid classes found in isolated PD and PM fractions from Arabidopsis suspension cells.

(**A**) HP-TLC analysis of neutral lipids showing that only traces of GluCer were detected in PD or PM extracts (arrow) (ASG: acylated sterol glucosides; SG: sterol glucosides; X:unidentified lipid).

(**B**) HP-TLC analysis of GIPC series from PD and PM extracts. Note that GIPC from series A and series B are the most prominent classes found in PD and PM extracts. Inset, the table shows GIPC contents quantified by densitometric scanning. n=3 for PM and PD.

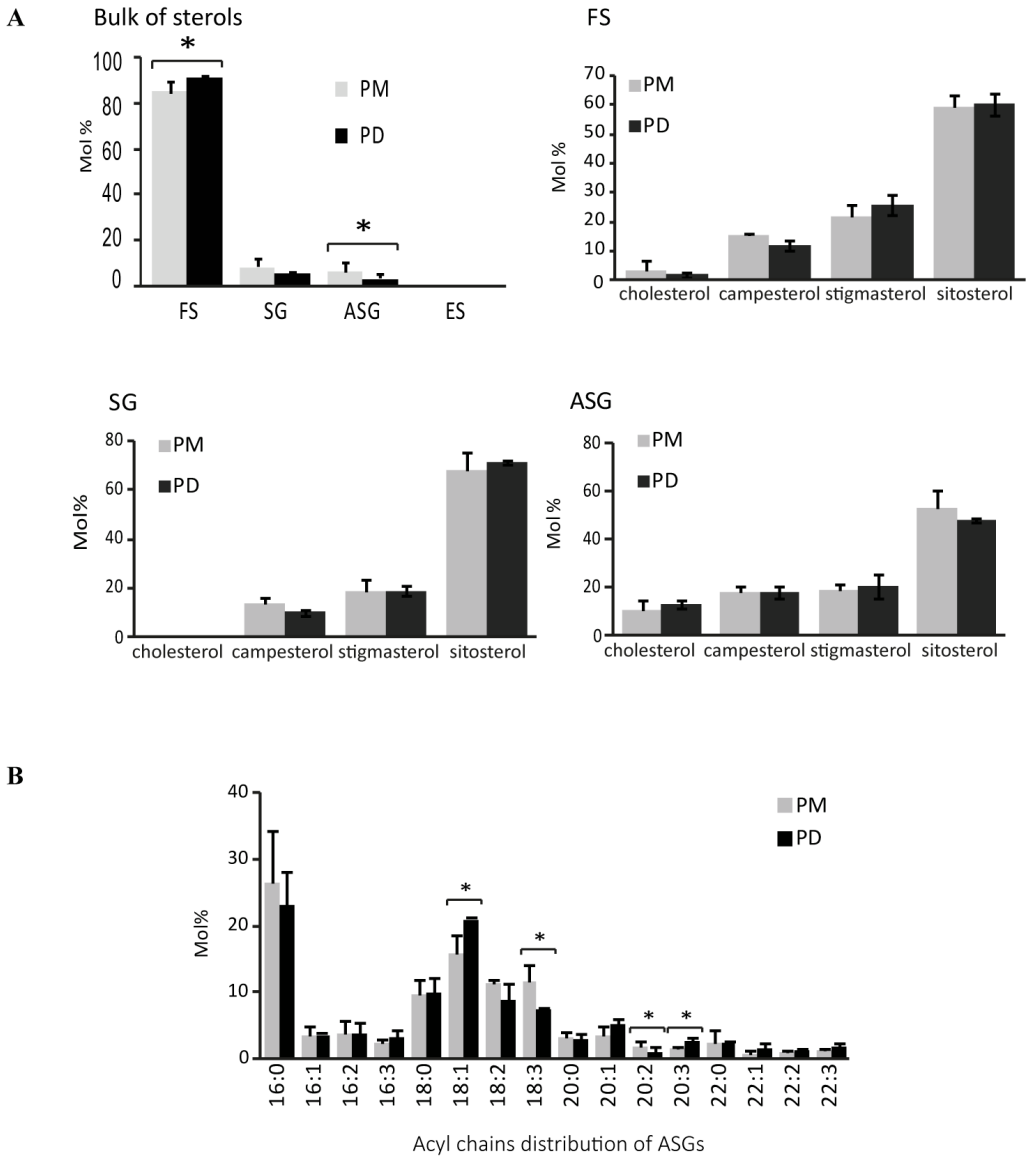

Supplemental Figure 10.

The molecular species distribution of sterol lipid classes in isolated PD and PM fractions is similar. Sterol molecular species were determined by Q-TOF MS/MS analyses.

(**A**) Free sterols (FS) and conjugated sterols ((sterol glucosides (SG) and acylated sterol glucosides (ASG)) are equally distributed in PD and PM fractions. Sterol esters were not detected (not shown).

(**B**) The fatty acid composition of ASG.

Asterisks indicate a significant difference ($P < 0.05$) between two samples by Annova of Kruskal-Wallis test. n=3 for PD and n=4 for PM. (n=3 for all samples). Bars indicate SD.

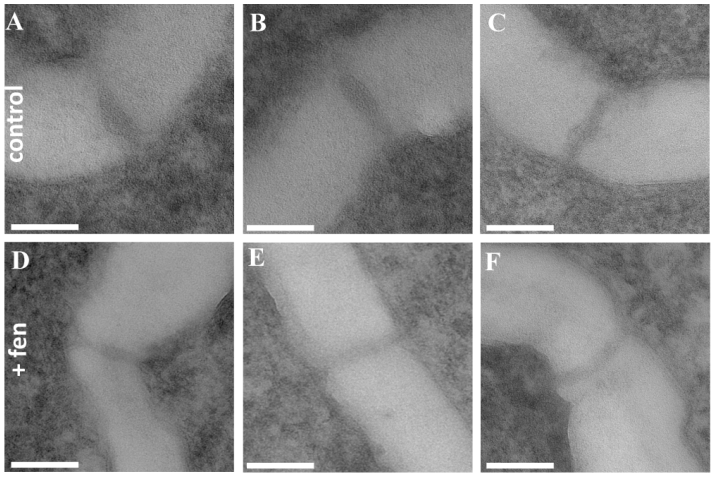

Supplemental Figure 11.

Electron micrograph of cryofixed Arabidopsis roots treated with fenpropimorph for 24 h.

PD from fen treated (24 h with 50 µg/mL) (**D-F**) or control (**A-C**) plants showed no obvious ultrastructural differences in Arabidopsis roots epidermal cells. Scale Bars= 100 nm

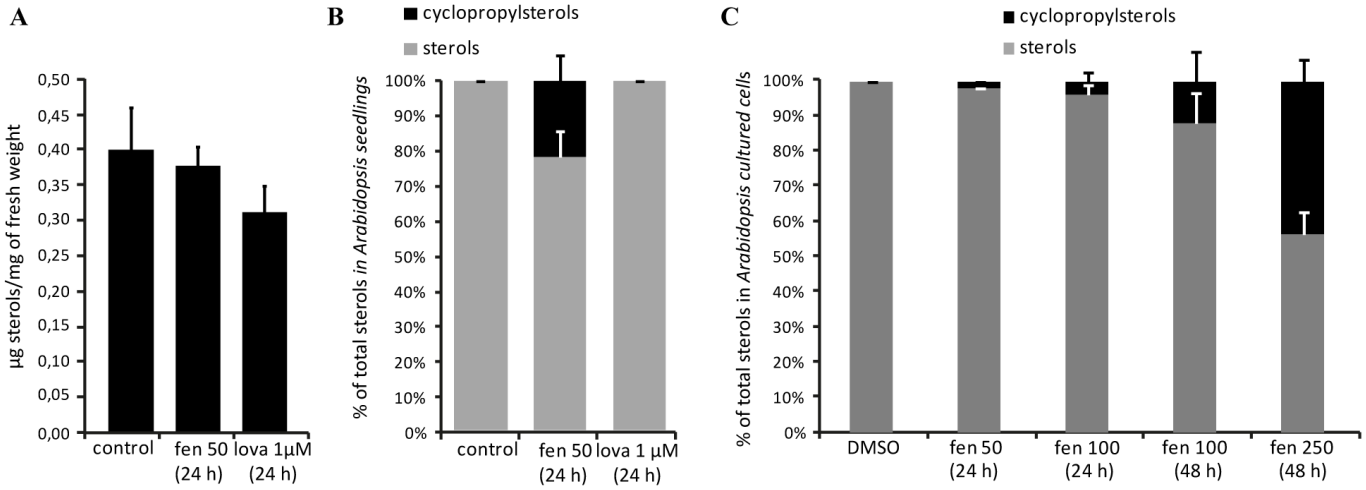

Supplemental Figure 12.

Sterol composition of lova and fen treated Arabidopsis seedlings and cultured cells.

(**A-B**) Total amount of sterols (A) and relative proportion of sterols and cyclopropyl sterols (B) in *Arabidopsis* seedlings treated with either fenpropimorph (fen) or lovastatin (lova) for 24 h. n=2. Bars indicate SD.

(**C**) Relative proportion of sterols and cyclopropyl sterols in cultured cells treated with fen sterol inhibitor for different periods of time and concentrations.

fen50, 100, 250 correspond to concentration used in µg/mL. n=2. Bars indicate SD.

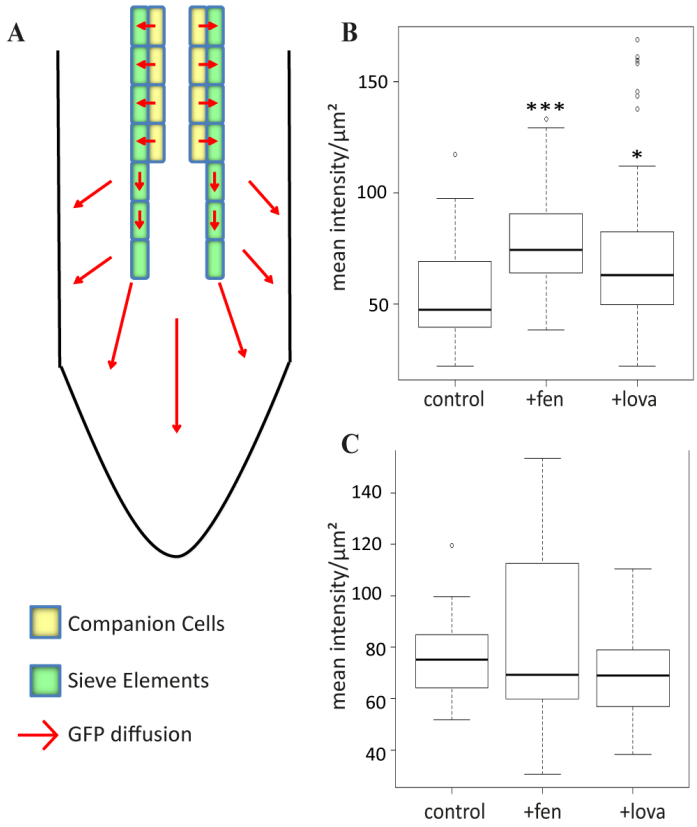

Supplemental Figure 13.

proSUC2:GFP intensity measurement in the vasculature of Arabidopsis roots treated with fen or lova for 24 h and 48 h.

(**A**) Schematic presentation of Arabidopsis root highlighting the phloem companion cells and sieve elements and the symplastic unloading zone of proSUC2::GFP from the companion cells to the root meristem and surrounding tissues. Adapted from Vaten *et al.* 2011.

(**B, C**) Quantification of GFP fluorescence in the root vasculature of fen and lova treated plants for 24 h (B) and 48 h (C). Experiments were performed at least three independent times using a total of 20 seedlings per condition. Asterisks indicate significant differences ($p<0.05$ one asterisk and $p<0.001$ for three asterisks) using Wilcoxon test. Bars indicate SD.

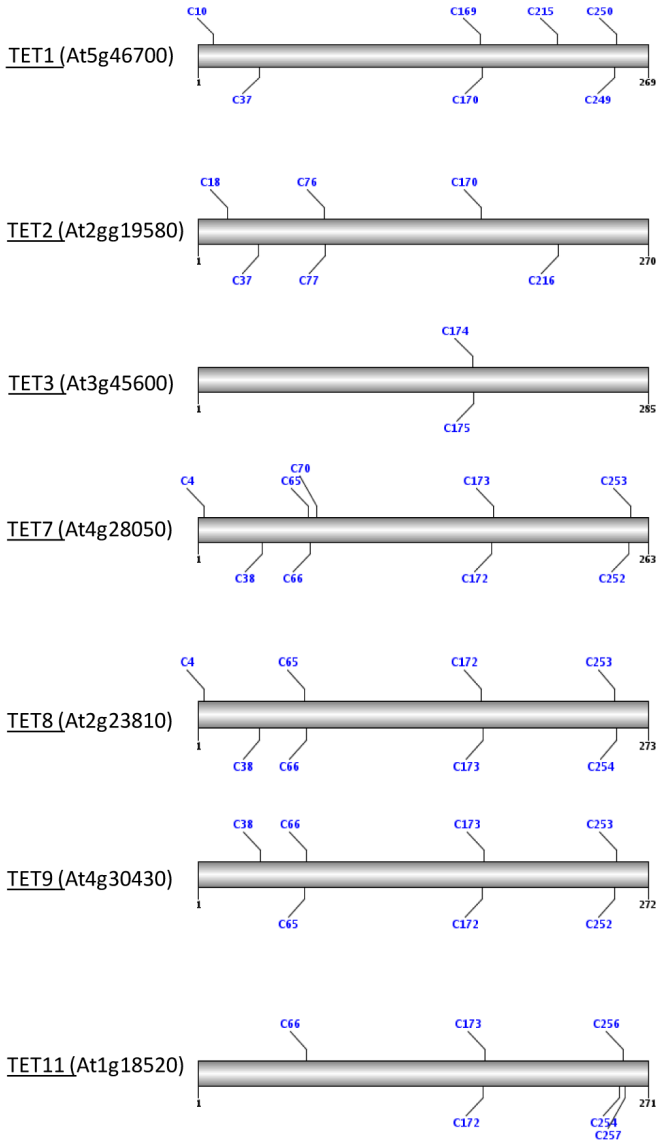

Supplemental Figure 14.

List of the tetraspanins identified in the PD proteome and their putative S-acylation sites.

The PD and PM fractions were analysed using an MS-based proteomic approach (n=3) and members of the tetraspanin family presenting an enrichment in the PD-enriched membrane fraction were identified (See Supplemental Table 1). Prediction of post-translational lipid modification S-acylation (palmitoylation) was performed using CSS-palm software version 4 with high threshold settings (http://csspalm.biocuckoo.org). All tetraspanin members enriched at PD contained multiple putative S-acylation sites. In mammalian, palmitoylation of tetraspanins has been suggested to be essential for direct interaction with sterols (Charrin et al., 2003).

Gene	Putative function	Peptide Count	Normalized abundance								Ratio	
			PM1	PM2	PM3	PM average	PD1	PD2	PD3	PD average	PD *vs* PM	PM *vs* PD
AT5G42100	beta-1,3-glucanase AtBG_PAP	22	479 011	203 368	285 766	322 715	28 689 288	14 711311	22 271900	21890 833	**68**	
AT3G13560	beta-1,3-glucanase PdBG1	9	31790	8 514	11662	17 322	280 801	81283	78 542	146 875,42	**8**	
AT2G01630	beta-1,3-glucanase PdBG2	8	59 119	19 129	66 482	48 243	504 613	1678 216	577 068	919 965,73	**19**	
AT5G61130	plasmodesmata callose-binding protein 1	5	62 060	50 070	42 672	51601	710 555	716 986	842 575	756 705,45	**15**	
AT1G69295	plasmodesmata callose-binding protein 4	5	8 083	2 416	7 330	5 943	421928	506 728	207 064	378 573,47	**64**	
AT3G58100	plasmodesmata callose-binding protein 5	2	29 789	16 102	24 715	23 535	435 718	648 600	359 249	481 188,93	**20**	
AT5G43980	plasmodesmata-located protein 1	18	52 200	49 025	46 545	49 257	2 320 133	612 927	637 877	1 190 312,62	**24**	
AT1G04520	plasmodesmata-located protein 2	7	7 797	11852	6 006	8 552	230 735	116 991	138 617	162 114,55	**19**	
AT2G33330	plasmodesmata-located protein 3	8	5 713	12 541	7 281	8 512	390 063	823 552	1026 415	746 676,69	**88**	
AT3G60720	plasmodesmata-located protein 8	2	2 412	1715	209	1445	59 303	15 516	24 238	33 019,06	**23**	
AT5G13000	glucan synthase-like 12 (Vaten et al.)	64	562 909	172 032	150 882	295 274	738 438	1058 565	634 223	810 408,76	**3**	
AT4G21380	receptorkinase3 (Calvino-Fernandez)	5	11 114	6 022	6 020	7 719	37 480	76 986	10 701	41722,23	**5**	
AT5G46700	tetraspanin1	11	182 081	125 421	72 867	126 790	720 133	709 982	856 515	762 209,98	**6**	
AT2G19580	tetraspanin2	3	35 182	10 500	8 172	17 951	313 299	301 180	159 504	257 994,13	**14**	
AT3G45600	tetraspanin3	9	42 733	27 389	10 263	26 795	377 033	208 541	223 256	269 609,92	**10**	
AT4G28050	tetraspanin7	6	24 834	5 932	15 800	15 522	187 976	94 286	103 768	128 676,87	**8**	
AT2G23810	tetraspanin8	9	64 239	62 021	84 805	70 355	570 949	768 498	816 525	718 657,35	**10**	
AT4G30430	tetraspanin9	1	2	-	134	68	2 554	9 800	9 392	7 248,71	**107**	
AT1G18520	tetraspanin11	3	647	941	424	671	18 404	16 318	24 413	19 711,85	**29**	
AT4G30190	H(+)-ATPase 2	26	1406535	2290913	1391704	1696384	63475	63856	64241	63857		**27**
AT2G18960	H(+)-ATPase 1	45	5010932	4867643	4828582	4902386	125092	240364	232597	199351		**25**
AT5G64740	cellulose synthase 6	2	4814	8295	4973	6027	211	357	217	262		**23**
AT4G20260	associated cation-binding	11	1292554	1898883	1291212	1494217	80806	76672	63312	73597		**20**
AT4G33430	BRI1-associated receptor kinase	6	132045	213147	75759	140317	5389	6362	8294	6682		**21**
AT5G62690	tubulin beta chain 2	5	388882	347472	312021	349458	8408	12869	26984	16087		**22**
AT2G18730	diacylglycerol kinase 3	12	634696	1089678	574622	766332	42859	32802	50111	41924		**18**
AT4G35100	plasma membrane intrinsic protein 3	3	1309906	1950291	692683	1317627	82537	206213	185625	158125		**8**
AT5G55730	FASCICLIN-like arabinogalactan 1	5	763120	1679492	727074	1056562	12741	9812	7970	10174		**104**
AT1G01620	plasma membrane intrinsic protein 1C	1	1116661	1162463	479441	919522	157396	324658	299709	260588		**4**
AT1G49340	Phosphatidylinositol 3- and 4-kinase family protein	21	179769	186056	67531	144452	2623	3332	3298	3084		**47**

Supplemental Table 1.

List of PD- and PM- associated proteins identified by proteomic analysis.

Identification of PD and PM proteins by LC-MS/MS analyses from PD- and PM-enriched membrane fractions. n=3 for PD and PM fraction. Ten micrograms of protein was analysed for each fractions.

Name	Gene	Putative function	Reference	PD localization reference	GPI	sterol dependant DIM association	DIM reference
AtBG-pap	**At5g42100**	GHL17	Bayer et al. 2006	Levy et al 2007	Yes	Yes	Kierszniowska et al. 2008
glucanase	**At5g58090**	GHL17	Fernandez-Calvino et al. 2011	Fernandez-Calvino et al. 2011	Yes	yes	Zauber et al. 2014; Kierszniowska et al. 2008
pdGB1	**At3g13560**	GHL17	Bayer et al. 2006	Benitez-Alfonso et al. 2013	Yes	Yes	Zauber et al. 2014; Kierszniowska et al. 2008
pdGB2	**At2g01630**	GHL17	Benitez-Alfonso et al. 2013	Benitez-Alfonso et al. 2013	Yes	nf	
pdGB3	**At1g66250**	GHL17	Benitez-Alfonso et al. 2013	Benitez-Alfonso et al. 2013	Yes	nf	
PDCB1	**At5g61130**	regulation callose binding protein		Simpson et al. 2009	Yes	nf	
PDCB2	**At5g08000**	regulation callose binding protein		Simpson et al. 2009	Yes	nf	
PDCB3	**At1g18650**	regulation callose binding protein		Simpson et al. 2009	Yes	nf	
PDCB like 4	**At1g69295**	callose binding protein like		Simpson et al. 2009	Yes	nf	
PDCB like 5	**At3g58100**	callose binding protein like		Simpson et al. 2009	Yes	Yes	Kierszniowska et al. 2008
LYM2	**At2g17120**	Chitin perception		Faulkner et al. 2013	Yes	Yes	Kierszniowska et al. 2008

Supplemental Table 2.

List of PD GPI-anchored proteins and their occurrence in DIM.

List of GPI-anchored proteins identified in proteomic analyses of PD-enriched membrane fractions. DIM: Detergent Insoluble Membrane. GPI: Glycosyl PhosphoInositol.

Supplemental References

Bayer, E.M., Bottrill, A.R., Walshaw, J., Vigouroux, M., Naldrett, M.J., Thomas, C.L., and Maule, A.J. (2006). Arabidopsis cell wall proteome defined using multidimensional protein identification technology. Proteomics **6,** 301-311.

Benitez-Alfonso, Y., Faulkner, C., Pendle, A., Miyashima, S., Helariutta, Y., and Maule, A. (2013). Symplastic intercellular connectivity regulates lateral root patterning. Dev Cell **26,** 136-147.

Charrin, S., Maniè, S., Thiele, C., Billard, M., Gerlier, D., Boucheix, C., and Rubinstein, E. (2003). A physical and functional link between cholesterol and tetraspanins Eur. J. Immunol. **33,** 2579-2489.

Faulkner, C., Petutschnig, E., Benitez-Alfonso, Y., Beck, M., Robatzek, S., Lipka, V., and Maule, A.J. (2013). LYM2-dependent chitin perception limits molecular flux via plasmodesmata. Proc Natl Acad Sci U S A **110,** 9166-9170.

Fernandez-Calvino, L., Faulkner, C., Walshaw, J., Saalbach, G., Bayer, E., Benitez-Alfonso, Y., and Maule, A. (2011). Arabidopsis plasmodesmal proteome. PLoS One **6,** e18880.

Kierszniowska, S., Seiwert, B., and Schulze, W.X. (2008). Definition of Arabidopsis sterol-rich membrane microdomains by differential treatment with methyl-beta-cyclodextrin and quantitative proteomics. Mol. Cell. Proteomics **8,** 612-623.

Levy, A., Erlanger, M., Rosenthal, M., and Epel, B.L. (2007). A plasmodesmata-associated beta-1,3-glucanase in Arabidopsis. Plant J **49,** 669-682.

Simpson, C., Thomas, C., Findlay, K., Bayer, E., and Maule, A.J. (2009). An Arabidopsis GPI-anchor plasmodesmal neck protein with callose binding activity and potential to regulate cell-to-cell trafficking. Plant Cell **21,** 581-594.

Vaten, A., Dettmer, J., Wu, S., Stierhof, Y.D., Miyashima, S., Yadav, S.R., Roberts, C.J., Campilho, A., Bulone, V., Lichtenberger, R., Lehesranta, S., Mahonen, A.P., Kim, J.Y., Jokitalo, E., Sauer, N., Scheres, B., Nakajima, K., Carlsbecker, A., Gallagher, K.L., and Helariutta, Y. (2011). Callose biosynthesis regulates symplastic trafficking during root development. Dev Cell **21,** 1144-1155.

Zauber, H., Burgos, A., Garapati, P., and Schulze, W.X. (2014). Plasma membrane lipid-protein interactions affect processes in sterol-biosynthesis mutants in *Arabidopsis thaliana*. Frontiers in Plant Science. **5,** Article 78**.**